

## Appendix D.

### Examples of Aerodynamic Design\* *Using tools from our software suite*

This appendix provides examples of the procedures and use of computational aerodynamics tools for aerodynamic design. We do this using the simple tools available on the website, listed in App. E. The focus is on aerodynamic analyses typical of early conceptual and preliminary design work. We include the B-2, comparisons of the Beech Starship and the Grumman X-29, and the YF-22 and YF-23 ATF candidate designs. The examples are provided in considerable detail. The input data sets almost always mimic the old card input styles, and require that the values in the data sets be placed in specific fields. Although students aren't used to this style, I don't see a problem, and it's an easy adjustment. When making calculations, it is always important to assess whether the code is giving the "right" answer—the infamous "sanity check." These examples should help students examine results in their own work. Finally, many aerospace engineers are heavy users of computational methods. Some will modify existing codes. But only a handful of graduates will develop entirely new algorithms and codes. The examples contained here depict the typical work of an aerodynamic designer.

#### **D.1 An Overview of Configuration Aerodynamics Requirements**

These case studies illustrate many of the issues facing configuration aerodynamicists, tying together a number of aspects of aerodynamic theory and applications that are covered in the course. The results obtained in the term projects described in this Appendix have been highly instructive both to the students and the teacher. They provided the students with an opportunity to examine real world problems. Portions of these examples have been discussed previously in an AIAA Paper.<sup>1</sup>

A key component of these case studies is the need to gather information. Students must read the literature, and get to know the sorts of reports that are available. This means using NASA and AIAA literature, as well as AGARD and news-type publications (*Aviation Week, Interavia, Air International, etc.*).

#### **D.2 Examine the B-2**

The B-2 was unveiled in late November of 1988. This example was used as a class project in spring 1989. The statement of the assignment is given here as Table D-1.

---

\* This is the first version of this Appendix. Further details will be added in the future.

**Table D-1. B-2 Study Questions**

Using the best available information (*Aviation Week*, *Flight International*, *Popular Science*, etc), analyze the B-2 and provide an evaluation of the aircraft. Include at least the following:

1. Develop a geometry model of the B-2 for use in analysis and design.
2. Estimate  $C_{D0}$  for the B-2.
3. Find and plot the spanload assuming an untwisted wing. What is the span  $e$  for this case?
4. Plot the section  $C_l$  distribution. Where will the wing stall first? Do you see a problem?
5. What would you do to improve the spanload? Plot and analyze a twist distribution that will improve  $e$ . Plot the new spanload and compute “ $e$ ”.
6. Estimate  $L/D_{max}$  and the  $C_L$  required to fly at  $L/D_{max}$ . Comment on the implications for the operation of the B-2. What can you say about the B-2 in comparison with conventional aircraft?.
7. Determine the neutral point of the B-2. Examine the available information, and estimate the static margin. Does your conclusion make sense?

Several other aspects of the design are required. For example, it also requires an estimate of the  $cg$  of the B-2, although this wasn't explicitly stated. Some students were surprised that the static margin required both the neutral point and the  $cg$ , since they weren't given the  $cg$ .

1. *Develop a geometry model of the B-2 for use in analysis and design.* Initial specific sources of information included the *Aviation Week* story,<sup>2</sup> and the first three-view, which appeared in *Air International*.<sup>3</sup> The three-view was important. The side view allowed the students to estimate the  $cg$  by assuming a 15° angle from the landing gear ground contact to the  $cg$  location. Figure D-1 shows a plan view from Jane's that was used based on the information available. The lecture by Waaland,<sup>4</sup> and the Aerofax book<sup>5</sup> were not yet available when this example was done.

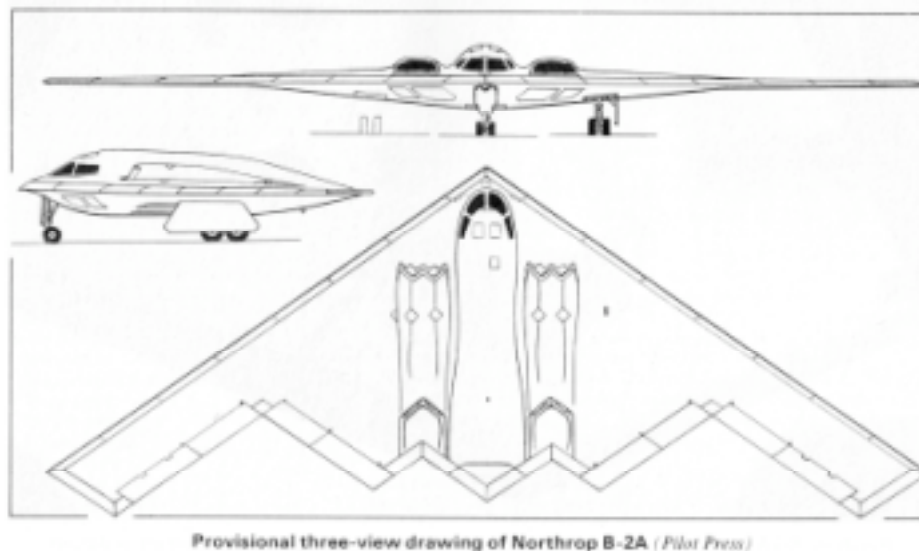


**Figure D-1 B-2 from Janes, 1990-91, (will have to get copyright permission)**

The numerical values of the so-called corner points measured from Fig. D-1, are show in Fig. D-2. Many students can't quite believe that engineers would be expected to scale a drawing to get quantitative values to develop a computational model. The integral properties were then found using the WingPlanAnal code. Table D-2 contains the input data set, and Table D-3 contains the output from the code.

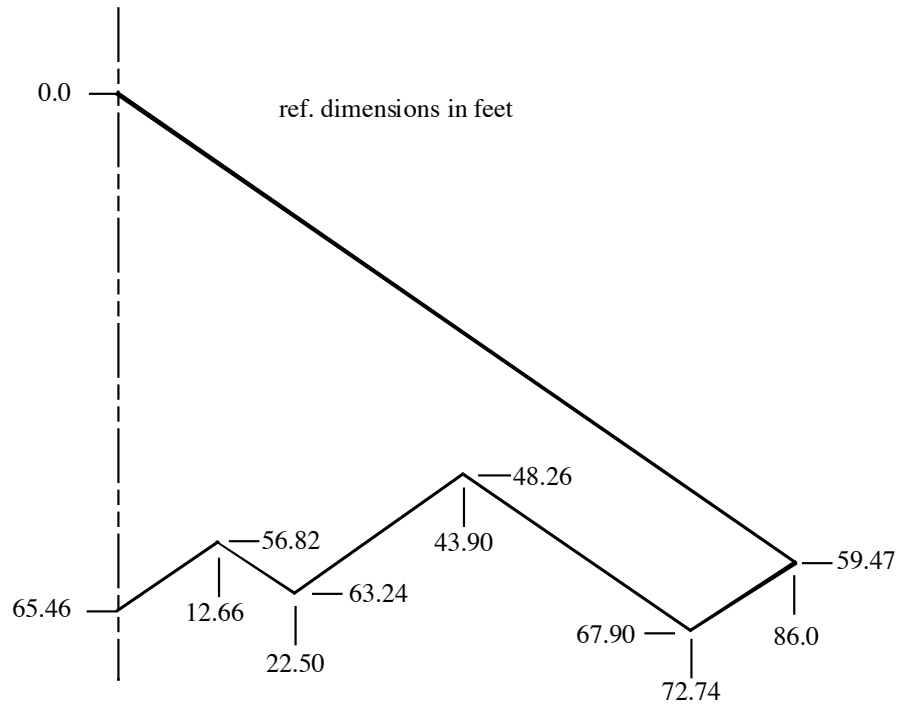


**Figure D-2. Idealization of B-2 for aerodynamic analysis**

**Table D-2 Input data set for WingPlanAnal**

```

B-2 Planform
2.0 Number of LE pts
YL      XL
  0.0    0.00
 86.0    59.47
6.0     Number of TE pts
YT      XT
 0.00   65.46
12.66   56.82
22.50   63.24
43.90   48.26
72.74   67.90
86.00   59.47
end of data
    
```

**Table D-3 WingPlanAnal output**

WingPlanAnal  
 Wing Planform Geometry Analysis  
 Virginia Tech Aircraft Design Software Series  
 W.H. Mason, Department of Aerospace and Ocean Engineering  
 Virginia Tech, Blacksburg, VA 24061, email: whmason@vt.edu  
 version: January 22, 2006  
 Planform Properties

Enter name of data set:

B2plan.inp

Input Case Title: B-2 Planform  
 Planform Points

Leading Edge		iLM = 2
i	YLE	XLE
1	0.0000	0.0000
2	86.0000	59.4700

Trailing Edge		iTM = 6
i	YTE	XTE
1	0.0000	65.4600
2	12.6600	56.8200
3	22.5000	63.2400
4	43.9000	48.2600
5	72.7400	67.9000
6	86.0000	59.4700

Interpolated LE and TE points and sweep

i	eta	y	XLE	LE sweep(deg)	XTE	TE sweep(deg)
0	0.000	0.000	0.000	34.664	65.460	-34.312
1	0.050	4.300	2.974	34.664	62.525	-34.312
2	0.100	8.600	5.947	34.664	59.591	-34.312

. . . *Intermediate values omitted to keep table to a single page* . . .

19	0.950	81.700	56.497	34.664	62.204	-32.446
20	1.000	86.000	59.470	34.664	59.470	-32.446

Integral Quantities

Planform Area	=	5039.31300
Mean Aerodynamic Chord	=	39.24220
X-Centroid	=	39.75905
Spanwise position of MAC	=	29.12163
X-Leading Edge of MAC	=	20.13795
Quarter Chord of MAC	=	29.94850
Aspect Ratio	=	5.87064
Average Chord	=	29.29833
Taper Ratio	=	0.00000

Note that the results found measuring the drawing are very close to the values for leading and trailing edge sweep angles given in the literature, which are 35°. Recall that this is a stealth airplane, using parallel edge alignment, see App. B. “Fifteen minutes of Stealth.”

## 2. Estimate $C_{D0}$ for the B-2

To estimate  $C_{D0}$ , the planform is broken up into strips, as shown in Figure D-3. The average chord of each strip, and the associated wetted area is then estimated. The option in WingPlanAnal to get the leading and trailing edge  $x$  values at a proscribed value of the span (not shown above) can be used to obtain this data.

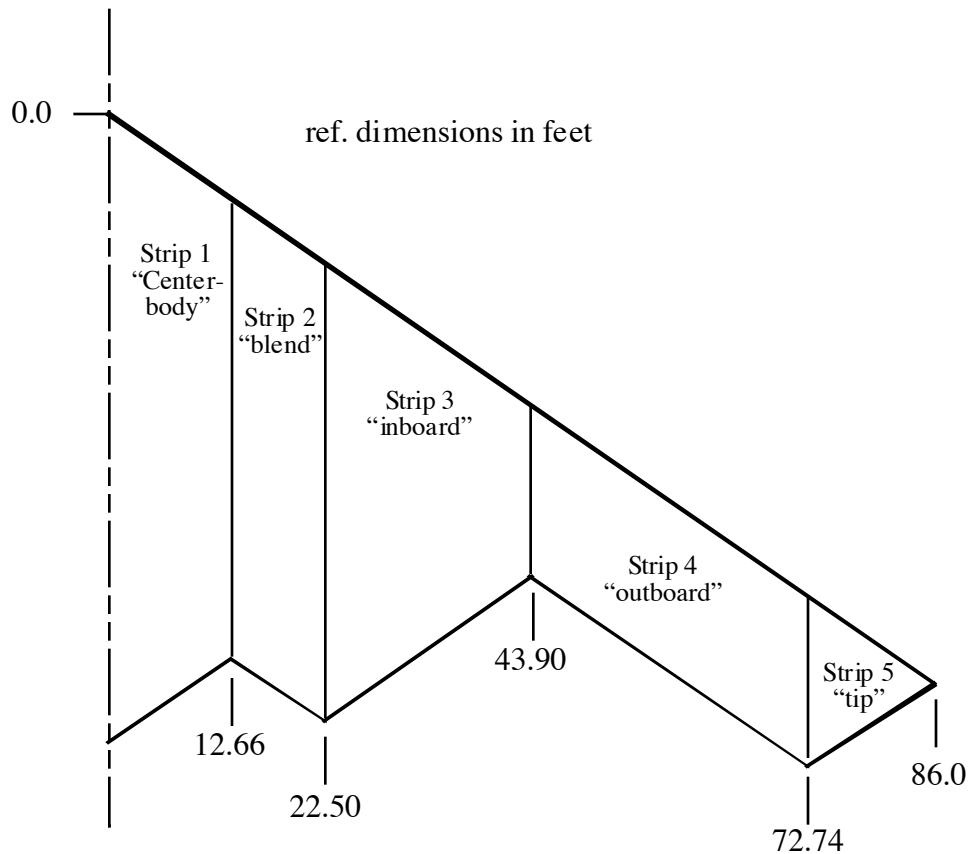


**Figure D-3. Strips used in making the skin friction estimate.**

With each of the strips being a trapezoid, some side calculations were made to find the area of each strip. This was then multiplied by four to include the top and bottom of the surface, as well as the area of the "other" side of the planform. The results are contained in the input data set for FRICTION, as given in Table D-4. It would be illustrative for students to compute the values contained in the Table for themselves.



**Table D-5. FRICTION output for the B-2 (continued).**

REYNOLDS NO./FT =0.308E+07    Altitude = 20000.00    XME = 0.780

COMPONENT	RN	CF	CF*SWET	CF*SWET*FF	CDCOMP
CenterBody	0.175E+09	0.00183	5.33262	11.01519	0.00218
Blending sectio	0.148E+09	0.00187	3.56296	5.33565	0.00106
Inboard Wing	0.101E+09	0.00197	5.59596	7.52510	0.00149
Outboard Wing	0.547E+08	0.00216	4.46050	5.99820	0.00119
Tip section	0.362E+08	0.00229	1.08127	1.31925	0.00026
		SUM =	20.03331	31.19339	0.00618

FRICTION DRAG: CDF = 0.00397

FORM DRAG: CDFORM = 0.00221

REYNOLDS NO./FT =0.172E+07    Altitude = 37000.00    XME = 0.780

COMPONENT	RN	CF	CF*SWET	CF*SWET*FF	CDCOMP
CenterBody	0.979E+08	0.00198	5.78279	11.94508	0.00237
Blending sectio	0.825E+08	0.00203	3.86697	5.79093	0.00115
Inboard Wing	0.565E+08	0.00215	6.08509	8.18284	0.00162
Outboard Wing	0.306E+08	0.00235	4.86635	6.54396	0.00130
Tip section	0.202E+08	0.00251	1.18243	1.44268	0.00029
		SUM =	21.78364	33.90549	0.00672

FRICTION DRAG: CDF = 0.00432

FORM DRAG: CDFORM = 0.00240

REYNOLDS NO./FT =0.149E+07    Altitude = 40000.00    XME = 0.780

COMPONENT	RN	CF	CF*SWET	CF*SWET*FF	CDCOMP
CenterBody	0.848E+08	0.00202	5.90243	12.19220	0.00242
Blending sectio	0.715E+08	0.00207	3.94782	5.91200	0.00117
Inboard Wing	0.490E+08	0.00219	6.21538	8.35805	0.00166
Outboard Wing	0.265E+08	0.00241	4.97476	6.68974	0.00133
Tip section	0.175E+08	0.00257	1.20950	1.47571	0.00029
		SUM =	22.24990	34.62771	0.00686

FRICTION DRAG: CDF = 0.00441

FORM DRAG: CDFORM = 0.00245

SUMMARY

J	XME	Altitude	RE/FT	CDF	CDFORM	CDF+CDFORM
1	0.400	0.000E+00	0.284E+07	0.00416	0.00232	0.00647
2	0.780	0.200E+05	0.308E+07	0.00397	0.00221	0.00618
3	0.780	0.370E+05	0.172E+07	0.00432	0.00240	0.00672
4	0.780	0.400E+05	0.149E+07	0.00441	0.00245	0.00686

END OF CASE

The values of skin friction are relatively low, reflecting the small multiplier of wetted to reference area, and rather large Reynolds numbers. Note that the value changes with altitude, where the Reynolds number decreases as the altitude increases, so that the skin friction increases.

3. Find and plot the spanload assuming an untwisted wing. What is the span  $e$  for this case?

To find the untwisted spanload, we start by using **VLMpc** to compute the spanload. This calculation will also provide other useful information. Table D-6 contains the input data set. The output of this code is rather lengthy, and we will provide the key parts of it As Table D-7.

**Table D-6 Input to VLMpc for the B-2**

```

ANALYSIS OF THE B-2: AIR INTERNATIONAL GEOMETRY
1.      1.      1.0000   5040.1   0.0
  6.      0.      0.      -0.00
    0.00    0.00    0.0      1.
-59.47   -86.00    0.      1.
-67.90   -72.74    0.      1.
-48.26   -43.90    0.      1.
-63.24   -22.50    0.      1.
-56.82   -12.66    0.      1.
-65.46    0.00
  1.  8. 20.  .30 1.  0.  0.  0.      0.      0.
end of data
    
```

**Table D-7. Output of VLMpc for the B-2**

```

vortex lattice aerodynamic computation program
nasa-lrc no. a2794 by j.e. lamar and b.b. gloss

modified for watfor77 with 72 column output

ANALYSIS OF THE B-2: AIR INTERNATIONAL GEOMETRY

      geometry data

      reference planform has  6 curves

center of gravity =  0.00000
root chord height =  0.00000
variable sweep pivot position   x(s) =  0.00000   y(s) =  0.00000

      break points for the reference planform

point      x      y      sweep      dihedral      move
          ref    ref    angle      angle         code

  1      0.00000    0.00000    34.66431    0.00000        1
  2     -59.47000   -86.00000   -32.44602    0.00000        1
  3     -67.90000   -72.74000    34.25482    0.00000        1
  4     -48.26000   -43.90000   -34.99203    0.00000        1
  5     -63.24000   -22.50000    33.12201    0.00000        1
  6     -56.82000   -12.66000   -34.31215    0.00000        1
  7     -65.46000    0.00000

      configuration no.      1.
    
```

curve 1 is swept 34.66431 degrees on planform 1

break points for this configuration

point	x	y	z	sweep angle	dihedral angle	move code
1	0.00000	0.00000	0.00000	34.66431	0.00000	1
2	-59.47000	-86.00000	0.00000	-32.44603	0.00000	1
3	-67.90000	-72.74000	0.00000	34.25482	0.00000	1
4	-48.26000	-43.90000	0.00000	-34.99203	0.00000	1
5	-63.24000	-22.50000	0.00000	33.12201	0.00000	1
6	-56.82000	-12.66000	0.00000	-34.31215	0.00000	1
7	-65.46000	0.00000	0.00000			

160 horseshoe vortices used on the left half of the configuration

planform	total	spanwise
1	160	20

8. horseshoe vortices in each chordwise row

aerodynamic data

configuration no. 1.

static longitudinal aerodynamic coefficients are computed

panel no.	x c/4	x 3c/4	y	z	s
1	-58.07243	-58.25077	-83.85000	0.00000	2.15000
2	-58.42913	-58.60748	-83.85000	0.00000	2.15000
3	-58.78583	-58.96418	-83.85000	0.00000	2.15000
4	-59.14253	-59.32088	-83.85000	0.00000	2.15000
5	-59.49923	-59.67758	-83.85000	0.00000	2.15000
6	-59.85593	-60.03428	-83.85000	0.00000	2.15000
7	-60.21263	-60.39098	-83.85000	0.00000	2.15000
8	-60.56933	-60.74768	-83.85000	0.00000	2.15000
9	-55.27727	-55.81232	-79.55000	0.00000	2.15000
10	-56.34737	-56.88243	-79.55000	0.00000	2.15000

*details for panels 11 – 150 omitted*

151	-48.76898	-52.32695	-6.21000	0.00000	2.15000
152	-55.88493	-59.44291	-6.21000	0.00000	2.15000
153	-3.36223	-7.27916	-2.03000	0.00000	2.03000
154	-11.19608	-15.11301	-2.03000	0.00000	2.03000
155	-19.02994	-22.94687	-2.03000	0.00000	2.03000
156	-26.86379	-30.78072	-2.03000	0.00000	2.03000
157	-34.69764	-38.61457	-2.03000	0.00000	2.03000



stat	2y/b	sl coef	cl ratio	c ratio	load dueto twist	add. load at cl = 0.000	basic load at cl = 0	span load at cl desir	x loc of local cent of press
1	-0.975	0.224	2.299	0.097	0.000	0.000	0.000	0.224	-58.722
2	-0.925	0.439	1.504	0.292	0.000	0.000	0.000	0.439	-57.045
3	-0.873	0.598	1.208	0.495	0.000	0.000	0.000	0.598	-55.211
4	-0.821	0.695	1.156	0.601	0.000	0.000	0.000	0.695	-52.827
5	-0.771	0.750	1.243	0.603	0.000	0.000	0.000	0.750	-50.026
6	-0.721	0.789	1.305	0.604	0.000	0.000	0.000	0.789	-47.160
7	-0.671	0.822	1.356	0.606	0.000	0.000	0.000	0.822	-44.263
8	-0.621	0.853	1.404	0.608	0.000	0.000	0.000	0.853	-41.360
9	-0.571	0.887	1.456	0.609	0.000	0.000	0.000	0.887	-38.476
10	-0.528	0.927	1.519	0.610	0.000	0.000	0.000	0.927	-36.068
11	-0.485	0.998	1.400	0.713	0.000	0.000	0.000	0.998	-34.280
12	-0.435	1.097	1.196	0.917	0.000	0.000	0.000	1.097	-32.620
13	-0.385	1.186	1.058	1.121	0.000	0.000	0.000	1.186	-30.966
14	-0.335	1.263	0.953	1.326	0.000	0.000	0.000	1.263	-29.311
15	-0.286	1.326	0.868	1.527	0.000	0.000	0.000	1.326	-27.677
16	-0.237	1.367	0.839	1.630	0.000	0.000	0.000	1.367	-25.683
17	-0.179	1.392	0.850	1.637	0.000	0.000	0.000	1.392	-22.972
18	-0.122	1.417	0.814	1.741	0.000	0.000	0.000	1.417	-20.779
19	-0.072	1.443	0.743	1.943	0.000	0.000	0.000	1.443	-19.562
20	-0.024	1.460	0.683	2.139	0.000	0.000	0.000	1.460	-18.598

induced drag, leading edge thrust , suction coefficient characteristics  
 computed at the desired cl from a near field solution

station	section coefficients				
	2y/b	l.e. sweep angle	cdii c/2b	ct c/2b	cs c/2b
1	-0.97500	34.66431	-0.00300	0.00777	0.00945
2	-0.92500	34.66431	-0.00216	0.01153	0.01402
3	-0.87291	34.66431	-0.00114	0.01386	0.01685
4	-0.82081	34.66431	-0.00070	0.01547	0.01880
5	-0.77081	34.66431	-0.00049	0.01645	0.02000
6	-0.72081	34.66431	-0.00058	0.01739	0.02114
7	-0.67081	34.66431	-0.00077	0.01828	0.02222
8	-0.62081	34.66431	-0.00094	0.01913	0.02325
9	-0.57081	34.66431	-0.00090	0.01983	0.02411
10	-0.52814	34.66431	0.00028	0.01952	0.02374
11	-0.48547	34.66431	0.00128	0.02005	0.02438
12	-0.43547	34.66431	0.00282	0.02053	0.02496
13	-0.38547	34.66431	0.00465	0.02059	0.02503
14	-0.33547	34.66431	0.00641	0.02047	0.02488
15	-0.28605	34.66431	0.00804	0.02014	0.02449
16	-0.23663	34.66431	0.00994	0.01913	0.02325
17	-0.17942	34.66431	0.01238	0.01728	0.02101
18	-0.12221	34.66431	0.01519	0.01501	0.01825
19	-0.07221	34.66431	0.01800	0.01274	0.01549
20	-0.02360	34.66431	0.02590	0.00522	0.00634

```

total coefficients
cdii/cl**2= 0.05620   ct= 0.19392   cs= 0.23577
end of file encountered after configuration 1.
    
```

The spanload results are shown in Figure D-4. For comparison, the elliptic spanload at the same lift coefficient is included.\*

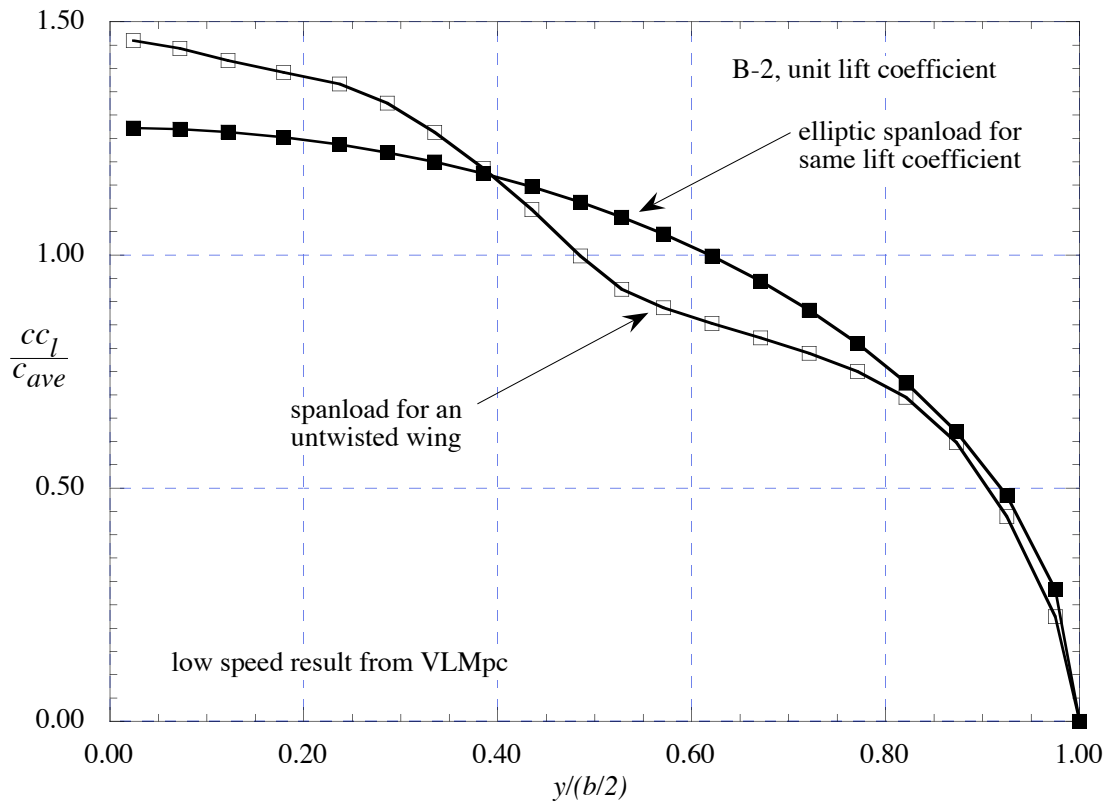


**Figure D-4. B-2 untwisted wing spanload compared with an elliptic (minimum induced drag) spanload**

With the basic spanload determined, we use **LIDRAG** to compute the span  $e$ . This code does a Fourier series analysis. Table D-8 contains the input data set, and Table D-9 provides the output of the program.

\* A useful relation is  $\frac{cc_l}{c_{avg}} = \frac{4}{\pi} \sqrt{1 - \eta^2} C_L$

**Table D-8 LIDRAG input for the B-2**

```

22.
0.000    1.461
0.024    1.460
0.072    1.443
0.122    1.417
0.179    1.392
0.237    1.367
0.286    1.326
0.335    1.263
0.385    1.186
0.435    1.097
0.485    0.998
0.528    0.927
0.571    0.887
0.621    0.853
0.671    0.822
0.721    0.789
0.771    0.750
0.821    0.695
0.873    0.598
0.925    0.439
0.975    0.224
1.0      0.000

```

**Table D-9. LIDRAG output for the B-2.**

```

Program LIDRAG
enter name of input data file
B2LIDRAG.inp
LIDRAG - LIFT INDUCED DRAG ANALYSIS

INPUT SPANLOAD
N      Y/(B/2)      CCLCA
1      0.00000     1.46100
2      0.02400     1.46000
3      0.07200     1.44300
4      0.12200     1.41700
5      0.17900     1.39200
6      0.23700     1.36700
7      0.28600     1.32600
8      0.33500     1.26300
9      0.38500     1.18600
10     0.43500     1.09700
11     0.48500     0.99800
12     0.52800     0.92700
13     0.57100     0.88700
14     0.62100     0.85300
15     0.67100     0.82200
16     0.72100     0.78900
17     0.77100     0.75000
18     0.82100     0.69500
19     0.87300     0.59800

```

**Table D-9. LIDRAG output for the B-2 (continued).**

	20	0.92500	0.43900
	21	0.97500	0.22400
	22	1.00000	0.00000
Span $e =$	0.94957	CL =	1.000
Press RETURN to quit the program.			

Using the results for the spanload obtained from the vortex lattice code, shown in Fig. D-4, a span  $e$  of 0.95 was found using **LIDRAG**. Considering the unusual planform, and the non-elliptic shape of the spanload, this is a surprisingly high value. Figure D-4 also contains the minimum induced drag (elliptic) spanload.

4. Plot the section  $C_l$  distribution. Where will the wing stall first? Do you see a problem?

The output from VLMpc also provides the section  $C_l$  distribution. This distribution is presented in Fig. D-5. This shows what happens when the planform has breaks leading to variations in the chord distribution. Because the spanload naturally tends toward a smooth distribution, the section lift coefficients vary to compensate for smaller chords by increasing. In addition, a pointed tip, where the chord goes to zero results in the local section lift coefficient becoming large. Locations where section  $C_l$ s are high would be locations where the wing would tend to stall first.

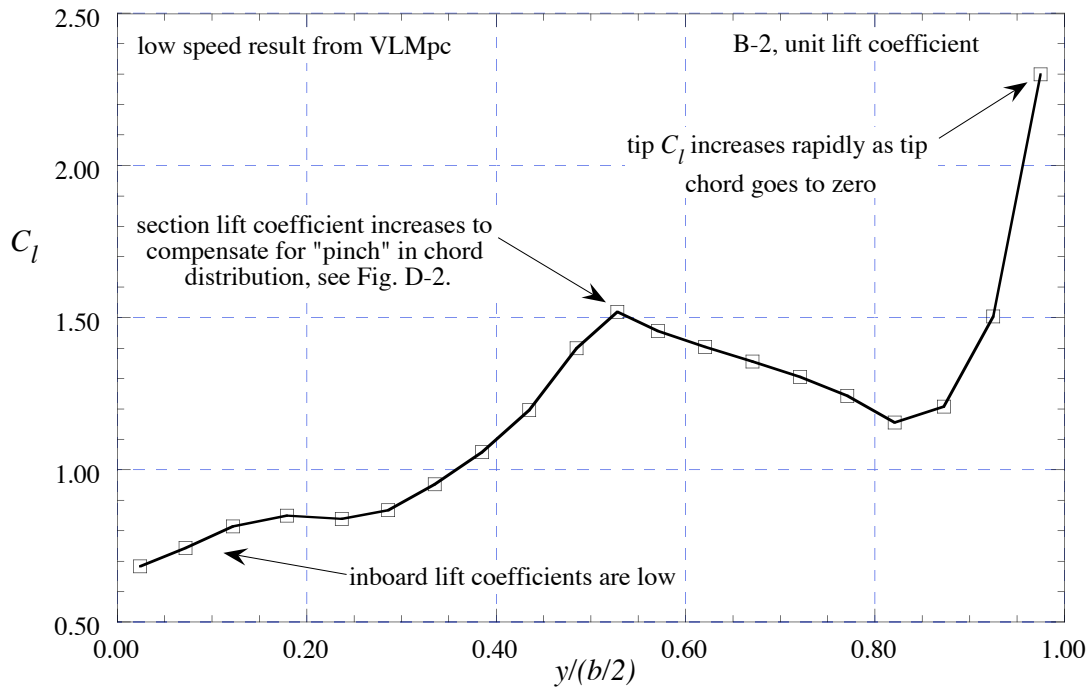


**Figure D-5. Spanwise section lift coefficient distribution for the B-2**

5. What would you do to improve the spanload? Plot and analyze a twist distribution that will improve  $e$ . Plot the new spanload and compute “ $e$ ”.

The **LAMDES** program can be used to find the twist distribution required to improve the spanload. Table D-10 contains the **LAMDES** input data set, which is quite similar to the **VLMpc** input. Table D-11 contains the corresponding output. Once again, the output is a lengthy text file, and relatively unimportant portions have been deleted.

**Table D-10 LAMDES input for the B-2**

```
LamarDesign Program - B-2 Planform -
  1.000  -0.000  39.24  5040.0  0.0  0.0  0.0
  6.      0.      0.      -0.00
  0.00    0.00    0.0    1.
-59.47   -86.00    0.      1.
-67.90   -72.74    0.      1.
-48.26   -43.90    0.      1.
-63.24   -22.50    0.      1.
-56.82   -12.66    0.      1.
-65.46    0.00
1.0 16.0 22. 0.78 0.34 40.0 0.0006
0.65    0.65    1.0    -0.00    1.0
0.030   1.0     0.0     0.0     0.0     0.0
```

**Table D-11 LAMDES output for the B-2**

enter name of input file:

B2LamDes.inp

Lamar Design Code mods by W.H. Mason

LamarDesign Program - B-2 Planform -

```
plan   = 1.0  xmref = 0.0000  cref   = 39.2400
tdklu  = 0.0  case  = 0.0      spnklu = 0.0
sref   = 5040.0000
```

```
REFERENCE PLANFORM HAS 6 CURVES
ROOT CHORD HEIGHT = 0.0000
```

POINT	X REF	Y REF	SWEEP ANGLE	DIHEDRAL ANGLE
1	0.0000	0.0000	34.66431	0.00000
2	-59.4700	-86.0000	-32.44602	0.00000
3	-67.9000	-72.7400	34.25482	0.00000
4	-48.2600	-43.9000	-34.99202	0.00000
5	-63.2400	-22.5000	33.12201	0.00000
6	-56.8200	-12.6600	-34.31215	0.00000
7	-65.4600	0.0000		

```
scw    = 16.0      vic = 22.0
xitmax = 40.0     epsmax = 0.00060
```

## D-16 Configuration Aerodynamics

---

CONFIGURATION NO. 1.  
delta ord shift for moment = 0.0000

CURVE 1 IS SWEEPED 34.6643 DEGREES ON PLANFORM 1

BREAK POINTS FOR THIS CONFIGURATION

POINT	X	Y	Z	SWEEP ANGLE	DIHEDRAL ANGLE
1	0.0000	0.0000	0.0000	34.6643	0.0000
2	-59.4700	-86.0000	0.0000	-32.4460	0.0000
3	-67.9000	-72.7400	0.0000	34.2548	0.0000
4	-48.2600	-43.9000	0.0000	-34.9920	0.0000
5	-63.2400	-22.5000	0.0000	33.1220	0.0000
6	-56.8200	-12.6600	0.0000	-34.3121	0.0000
7	-65.4600	0.0000	0.0000		

a = 0.000      clmin = 0.000      cd0 = 0.0000

336 HORSESHOE VORTICES USED

PLANFORM	TOTAL	SPANWISE
1	336	21

16. HORSESHOE VORTICES IN EACH CHORDWISE ROW

xcfw = 0.65      xcft = 0.65      fkon = 1.00  
ficam = 1.00      punch = 0.00      crbmnt = 0.000  
cmb = 0.00      iflag = 1

relax = 0.03      fioutw = 1.00      cd0 = 0.0000  
firbm = 0.00      yrbm = 0.0000      zrbm = 0.0000

LM = 50    IL = 51    JM = 51    IM = 53    TSPAN = -86.000    TSPANNA = 0.000  
BOTL = 86.000    BOL = 0.000    SNN = 0.8600    DELTYB = 1.7200  
NMA(KBOT) = 50    KBOT = 1    NMA(KBIT) = 0    KBIT = 2

induced drag cd = 0.00621      pressure drag cdpt = 0.00000

induced drag alone was minimized on this run

ref. chord = 39.240    c average = 29.3023    true area = 5040.115  
ref. area = 5040.000    b/2 = 86.0000    ref ar = 5.8698  
true ar = 5.8697    Mach number = 0.7800

first planform    cl = 0.34000    cm = -0.33786    cb = -0.07251

1st planform    CL = 0.3401    CDP = 0.0000    CM = -0.3381    CB = -0.0726  
2nd planform    CL = 0.0000    CDP = 0.0000    CM = 0.0000    CB = 0.0000

no pitching moment or bending moment constraints

CL DES = 0.34000    CL COMPUTED = 0.3401    CM = -0.3381  
CD I = 0.00621    E = 1.0106  
CDPRESS = 0.00000    CDTOTAL = 0.00621

first planform

Y	CL*C/CAVE	C/CAVE	CL	CD
-84.0455	0.09965	0.08854	1.12552	0.00000
-80.1364	0.16140	0.26559	0.60769	0.00000
-75.4609	0.20992	0.47737	0.43974	0.00000
-70.7854	0.24711	0.60132	0.41094	0.00000
-66.8764	0.27281	0.60272	0.45264	0.00000
-62.9673	0.29506	0.60412	0.48841	0.00000
-59.0582	0.31449	0.60552	0.51936	0.00000
-55.1491	0.33163	0.60693	0.54641	0.00000
-51.2400	0.34686	0.60833	0.57019	0.00000
-46.5927	0.36277	0.60999	0.59472	0.00000
-41.9455	0.37662	0.70378	0.53513	0.00000
-38.0364	0.38678	0.88942	0.43487	0.00000
-34.1273	0.39574	1.07505	0.36811	0.00000
-30.2182	0.40357	1.26069	0.32012	0.00000
-25.3818	0.41176	1.49035	0.27628	0.00000
-20.5455	0.41840	1.62981	0.25672	0.00000
-16.6364	0.42271	1.63503	0.25853	0.00000
-13.6709	0.42533	1.63898	0.25951	0.00000
-10.7055	0.42745	1.73198	0.24680	0.00000
-6.7964	0.42943	1.91527	0.22422	0.00000
-2.4209	0.43063	2.12044	0.20309	0.00000

mean camber lines to obtain the spanload

(subsonic linear theory)

$y = -84.0455$        $y/(b/2) = -0.9773$       chord = 2.5943

slopes,  $dz/dx$ , at control points, from front to rear

x/c	dz/dx
0.0469	0.2086
0.1094	0.1308
0.1719	0.0843
0.2344	0.0521
0.2969	0.0281
0.3594	0.0090
0.4219	-0.0074
0.4844	-0.0233
0.5469	-0.0412
0.6094	-0.0655
0.6719	-0.1123
0.7344	-0.1436
0.7969	-0.1644
0.8594	-0.1777
0.9219	-0.1812
0.9844	-0.1643

## D-18 Configuration Aerodynamics

---

mean camber shape (interpolated to 41 points)

x/c	z/c	delta x	delta z	(z-zle)/c
0.0000	-0.0297	0.0000	-0.0772	0.0000
0.0250	-0.0350	0.0649	-0.0908	-0.0060
0.0500	-0.0403	0.1297	-0.1045	-0.0120
0.0750	-0.0451	0.1946	-0.1171	-0.0176
0.1000	-0.0492	0.2594	-0.1276	-0.0224
0.1250	-0.0524	0.3243	-0.1359	-0.0264
0.1500	-0.0550	0.3891	-0.1427	-0.0297
0.1750	-0.0572	0.4540	-0.1485	-0.0327
0.2000	-0.0591	0.5189	-0.1534	-0.0353
0.2250	-0.0607	0.5837	-0.1575	-0.0376
0.2500	-0.0620	0.6486	-0.1608	-0.0397
0.2750	-0.0630	0.7134	-0.1634	-0.0414
0.3000	-0.0638	0.7783	-0.1654	-0.0429
0.3250	-0.0643	0.8432	-0.1669	-0.0443
0.3500	-0.0647	0.9080	-0.1679	-0.0454
0.3750	-0.0649	0.9729	-0.1684	-0.0463
0.4000	-0.0650	1.0377	-0.1685	-0.0471
0.4250	-0.0648	1.1026	-0.1682	-0.0477
0.4500	-0.0646	1.1674	-0.1675	-0.0482
0.4750	-0.0641	1.2323	-0.1663	-0.0485
0.5000	-0.0635	1.2972	-0.1648	-0.0486
0.5250	-0.0627	1.3620	-0.1627	-0.0486
0.5500	-0.0618	1.4269	-0.1602	-0.0484
0.5750	-0.0606	1.4917	-0.1573	-0.0480
0.6000	-0.0593	1.5566	-0.1537	-0.0474
0.6250	-0.0576	1.6214	-0.1493	-0.0464
0.6500	-0.0554	1.6863	-0.1438	-0.0450
0.6750	-0.0528	1.7512	-0.1369	-0.0431
0.7000	-0.0497	1.8160	-0.1290	-0.0408
0.7250	-0.0464	1.8809	-0.1203	-0.0382
0.7500	-0.0428	1.9457	-0.1109	-0.0353
0.7750	-0.0389	2.0106	-0.1009	-0.0322
0.8000	-0.0349	2.0754	-0.0904	-0.0289
0.8250	-0.0307	2.1403	-0.0795	-0.0255
0.8500	-0.0263	2.2052	-0.0683	-0.0219
0.8750	-0.0219	2.2700	-0.0567	-0.0181
0.9000	-0.0173	2.3349	-0.0449	-0.0143
0.9250	-0.0128	2.3997	-0.0331	-0.0105
0.9500	-0.0083	2.4646	-0.0216	-0.0068
0.9750	-0.0041	2.5294	-0.0107	-0.0034
1.0000	0.0000	2.5943	0.0000	0.0000

y= -80.1364      y/(b/2) = -0.9318      chord= 7.7825

slopes, dz/dx, at control points, from front to rear

x/c	dz/dx
0.0469	0.1194
0.1094	0.0777
0.1719	0.0524
0.2344	0.0340
0.2969	0.0193
0.3594	0.0067

0.4219	-0.0049
0.4844	-0.0165
0.5469	-0.0292
0.6094	-0.0450
0.6719	-0.0725
0.7344	-0.0910
0.7969	-0.1033
0.8594	-0.1110
0.9219	-0.1131
0.9844	-0.1042

mean camber shape (interpolated to 41 points)

x/c	z/c	delta x	delta z	(z-zle)/c
0.0000	-0.0204	0.0000	-0.1587	0.0000
0.0250	-0.0234	0.1946	-0.1821	-0.0035
0.0500	-0.0264	0.3891	-0.2056	-0.0070
0.0750	-0.0292	0.5837	-0.2273	-0.0104
0.1000	-0.0316	0.7783	-0.2456	-0.0132
0.1250	-0.0335	0.9728	-0.2604	-0.0156
0.1500	-0.0351	1.1674	-0.2728	-0.0177
0.1750	-0.0364	1.3619	-0.2835	-0.0196
0.2000	-0.0376	1.5565	-0.2928	-0.0213
0.2250	-0.0386	1.7511	-0.3006	-0.0228
0.2500	-0.0395	1.9456	-0.3071	-0.0242
0.2750	-0.0401	2.1402	-0.3123	-0.0254
0.3000	-0.0407	2.3348	-0.3165	-0.0264
0.3250	-0.0411	2.5293	-0.3196	-0.0273
0.3500	-0.0413	2.7239	-0.3218	-0.0281
0.3750	-0.0415	2.9184	-0.3230	-0.0288
0.4000	-0.0415	3.1130	-0.3232	-0.0293
0.4250	-0.0415	3.3076	-0.3226	-0.0297
0.4500	-0.0413	3.5021	-0.3211	-0.0300
0.4750	-0.0409	3.6967	-0.3187	-0.0302
0.5000	-0.0405	3.8913	-0.3153	-0.0303
0.5250	-0.0400	4.0858	-0.3110	-0.0303
0.5500	-0.0393	4.2804	-0.3057	-0.0301
0.5750	-0.0385	4.4750	-0.2994	-0.0298
0.6000	-0.0375	4.6695	-0.2920	-0.0294
0.6250	-0.0364	4.8641	-0.2829	-0.0287
0.6500	-0.0349	5.0586	-0.2718	-0.0278
0.6750	-0.0332	5.2532	-0.2585	-0.0266
0.7000	-0.0313	5.4478	-0.2433	-0.0251
0.7250	-0.0291	5.6423	-0.2266	-0.0235
0.7500	-0.0268	5.8369	-0.2088	-0.0217
0.7750	-0.0244	6.0315	-0.1899	-0.0198
0.8000	-0.0219	6.2260	-0.1701	-0.0178
0.8250	-0.0192	6.4206	-0.1496	-0.0157
0.8500	-0.0165	6.6152	-0.1285	-0.0134
0.8750	-0.0137	6.8097	-0.1068	-0.0112
0.9000	-0.0109	7.0043	-0.0847	-0.0088
0.9250	-0.0080	7.1988	-0.0626	-0.0065
0.9500	-0.0053	7.3934	-0.0410	-0.0043
0.9750	-0.0026	7.5880	-0.0203	-0.0021
1.0000	0.0000	7.7825	0.0000	0.0000

*The similar results at each spanwise station are omitted here*

$y = -2.4209$        $y/(b/2) = -0.0282$       chord = 62.1337  
 slopes,  $dz/dx$ , at control points, from front to rear  

x/c	dz/dx
0.0469	-0.0098
0.1094	-0.0248
0.1719	-0.0325
0.2344	-0.0367
0.2969	-0.0390
0.3594	-0.0402
0.4219	-0.0406
0.4844	-0.0407
0.5469	-0.0410
0.6094	-0.0422
0.6719	-0.0476
0.7344	-0.0509
0.7969	-0.0533
0.8594	-0.0554
0.9219	-0.0569
0.9844	-0.0554

mean camber shape (interpolated to 41 points)

x/c	z/c	delta x	delta z	(z-zle)/c
0.0000	-0.0410	0.0000	-2.5464	0.0000
0.0250	-0.0407	1.5533	-2.5318	-0.0008
0.0500	-0.0405	3.1067	-2.5173	-0.0016
0.0750	-0.0402	4.6600	-2.4978	-0.0023
0.1000	-0.0397	6.2134	-2.4684	-0.0028
0.1250	-0.0391	7.7667	-2.4291	-0.0032
0.1500	-0.0384	9.3201	-2.3834	-0.0035
0.1750	-0.0376	10.8734	-2.3341	-0.0038
0.2000	-0.0367	12.4267	-2.2819	-0.0039
0.2250	-0.0358	13.9801	-2.2270	-0.0041
0.2500	-0.0349	15.5334	-2.1697	-0.0042
0.2750	-0.0340	17.0868	-2.1107	-0.0043
0.3000	-0.0330	18.6401	-2.0504	-0.0043
0.3250	-0.0320	20.1935	-1.9892	-0.0044
0.3500	-0.0310	21.7468	-1.9273	-0.0044
0.3750	-0.0300	23.3001	-1.8648	-0.0044
0.4000	-0.0290	24.8535	-1.8020	-0.0044
0.4250	-0.0280	26.4068	-1.7390	-0.0044
0.4500	-0.0270	27.9602	-1.6759	-0.0044
0.4750	-0.0260	29.5135	-1.6127	-0.0044
0.5000	-0.0249	31.0669	-1.5495	-0.0044
0.5250	-0.0239	32.6202	-1.4860	-0.0044
0.5500	-0.0229	34.1735	-1.4224	-0.0045
0.5750	-0.0219	35.7269	-1.3588	-0.0045
0.6000	-0.0208	37.2802	-1.2946	-0.0044
0.6250	-0.0198	38.8336	-1.2287	-0.0044
0.6500	-0.0187	40.3869	-1.1597	-0.0043
0.6750	-0.0175	41.9403	-1.0870	-0.0042
0.7000	-0.0163	43.4936	-1.0114	-0.0040

0.7250	-0.0150	45.0470	-0.9337	-0.0038
0.7500	-0.0137	46.6003	-0.8543	-0.0035
0.7750	-0.0124	48.1536	-0.7735	-0.0032
0.8000	-0.0111	49.7070	-0.6912	-0.0029
0.8250	-0.0098	51.2603	-0.6076	-0.0026
0.8500	-0.0084	52.8137	-0.5227	-0.0023
0.8750	-0.0070	54.3670	-0.4365	-0.0019
0.9000	-0.0056	55.9204	-0.3489	-0.0015
0.9250	-0.0042	57.4737	-0.2607	-0.0011
0.9500	-0.0028	59.0270	-0.1728	-0.0007
0.9750	-0.0014	60.5804	-0.0861	-0.0004
1.0000	0.0000	62.1337	0.0000	0.0000

twist table

i	y	y/(b/2)	twist
1	-84.04546	-0.97727	1.70360
2	-80.13635	-0.93182	1.16809
3	-75.46091	-0.87745	0.30947
4	-70.78545	-0.82309	-0.00569
5	-66.87636	-0.77763	0.68299
6	-62.96726	-0.73218	1.08198
7	-59.05817	-0.68672	1.41865
8	-55.14908	-0.64127	1.77459
9	-51.23998	-0.59581	2.21565
10	-46.59272	-0.54178	3.50599
11	-41.94546	-0.48774	3.90543
12	-38.03636	-0.44228	2.57660
13	-34.12727	-0.39683	2.07071
14	-30.21818	-0.35137	1.70050
15	-25.38182	-0.29514	1.16032
16	-20.54545	-0.23890	1.13859
17	-16.63636	-0.19345	2.12305
18	-13.67091	-0.15896	3.17933
19	-10.70545	-0.12448	2.84199
20	-6.79636	-0.07903	2.37425
21	-2.42091	-0.02815	2.34680

STOP

Figure D-6, shows the twist distribution required to obtain the minimum drag spanload. This was found using the constant chord-loading approach in **LAMDES**, which may not be a good assumption for this planform. However, the results are consistent with the changes in spanload required to achieve the  $e = 1$  elliptic spanload shown in Fig. D-4.

The section lift coefficient distribution is shown in Fig. D-5. Assuming that the small chord tip section  $C_l$ 's will be dominated by viscous effects in general, we see that wing stall will also occur in the midspan area. To fill in the hole in the spanload for the untwisted wing, the optimized twist distribution actually increases the local lift coefficient. The potential stall problem would be a reason to accept the  $e = .95$  spanload, without attempting to completely fill in the spanload distribution.

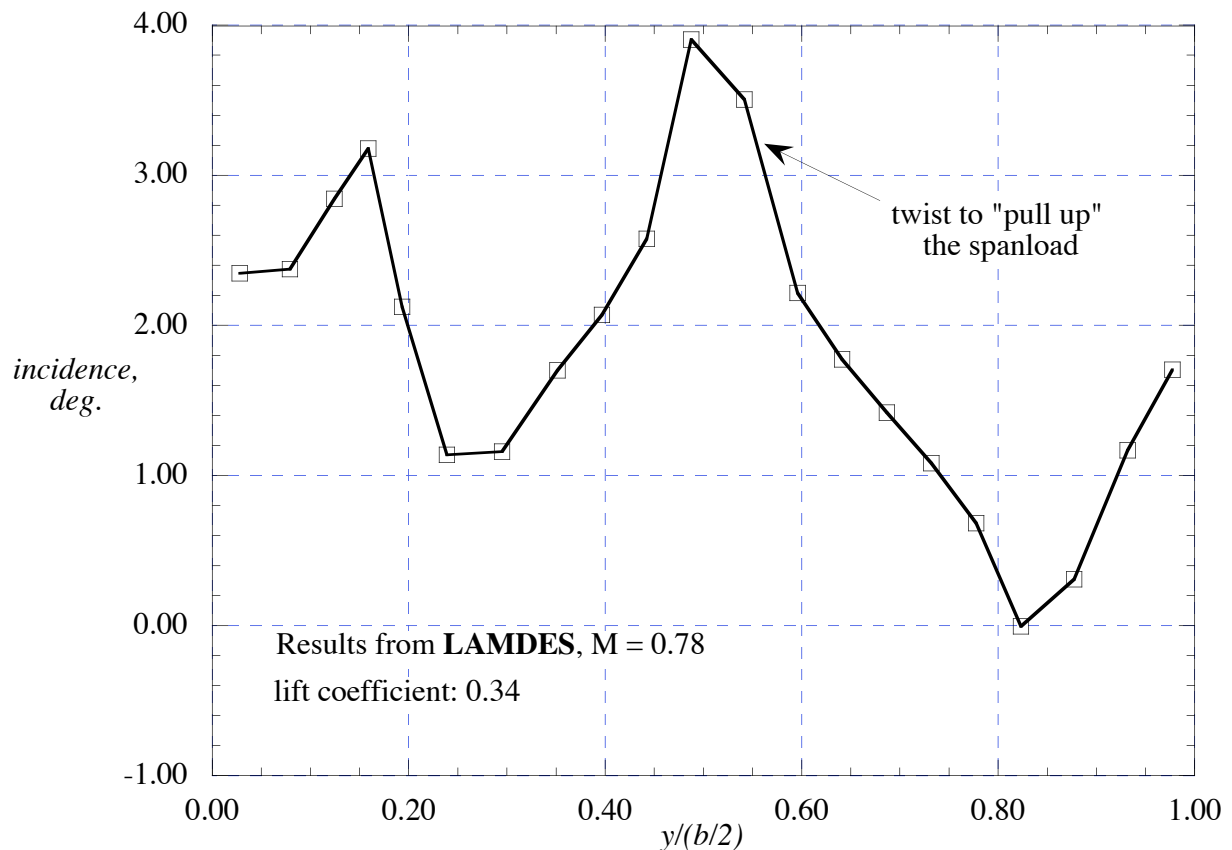


**Fig. D-6. B-2 incidence distribution required for minimum induced drag.**

6. Estimate  $L/D_{max}$  and the  $C_L$  required to fly at  $L/D_{max}$ . Comment on the implications for the operation of the B-2. What can you say about the B-2 in comparison with conventional aircraft?

Using the results from **FRICITION** and the spanload data analysis results from **LIDRAG**, we can make an estimate of the  $L/D$  variation with altitude. First, we provide the  $C_L$  requirement as the altitude increases, and then the  $L/D$  variation with altitude. This plot assumes  $M = 0.78$ , and the weight corresponds to the published value of 336,000 lbs. The lift coefficients in the cruise altitude range of 30 to 40,000 feet is relatively low compared to typical commercial transports. This is typical of flying wing aircraft. Figure D-8 contains the  $L/D$  variation for two different values of  $C_{D0}$ . Based on the results presented in Table D-5, The  $C_{D0}$  value of 80 counts is likely close to the value for the B-2, and agrees with the published result of a cruise altitude of 37,000 ft. The value of  $L/D$  max slightly greater than 21 is higher than typical commercial transonic transports. Indeed the B-2 is a very efficient airplane.

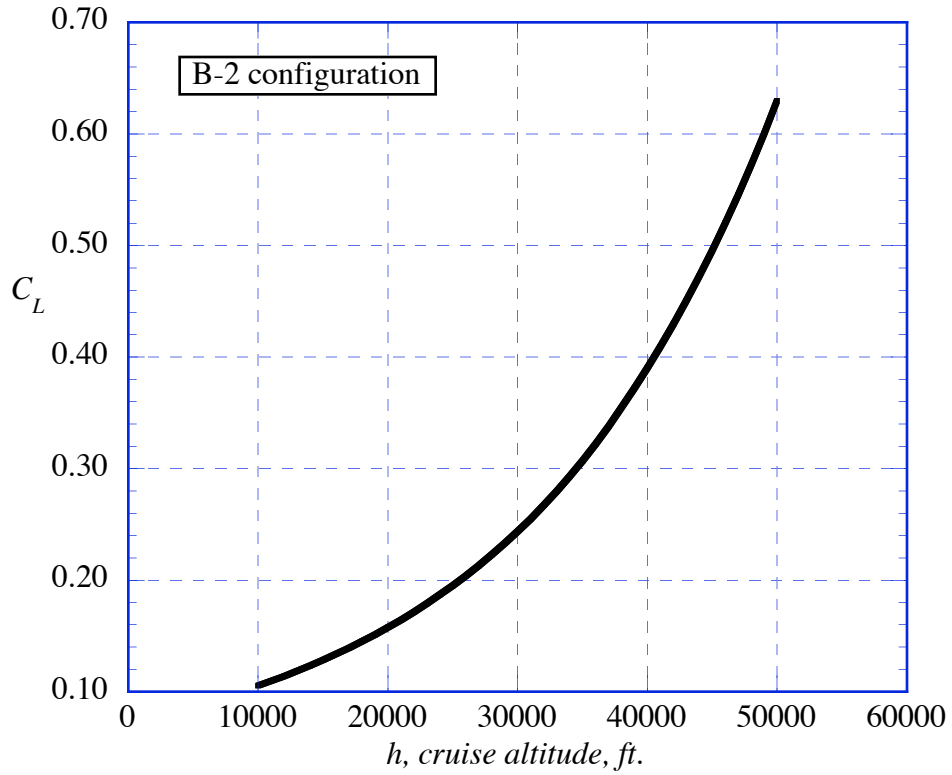


**Figure. D-7  $C_L$  variation with altitude**

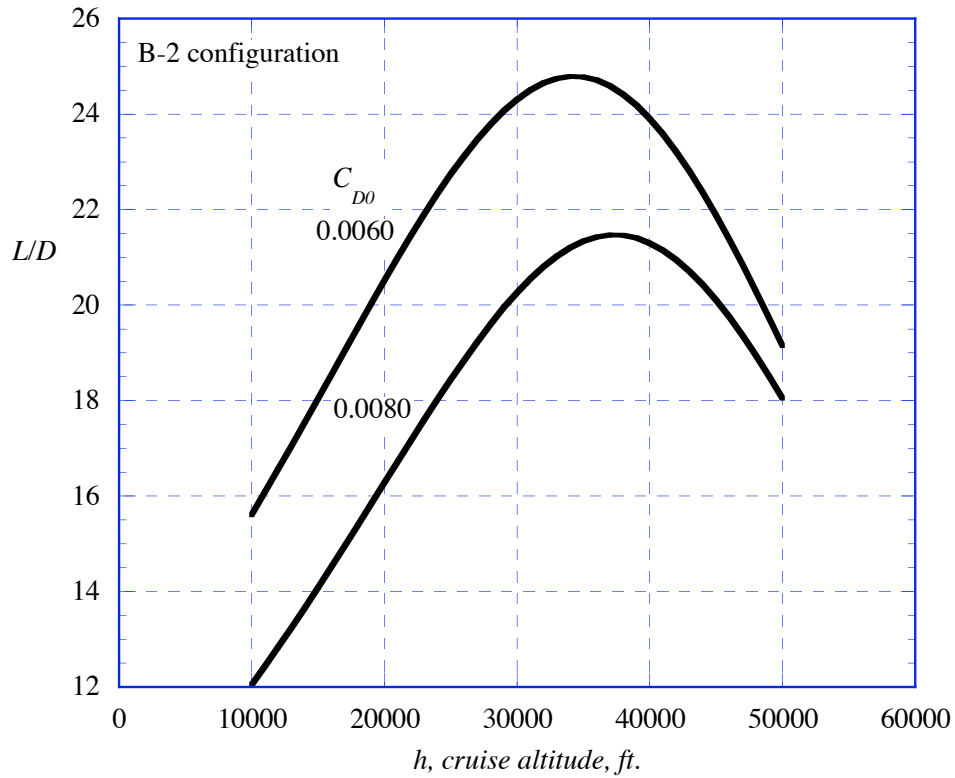
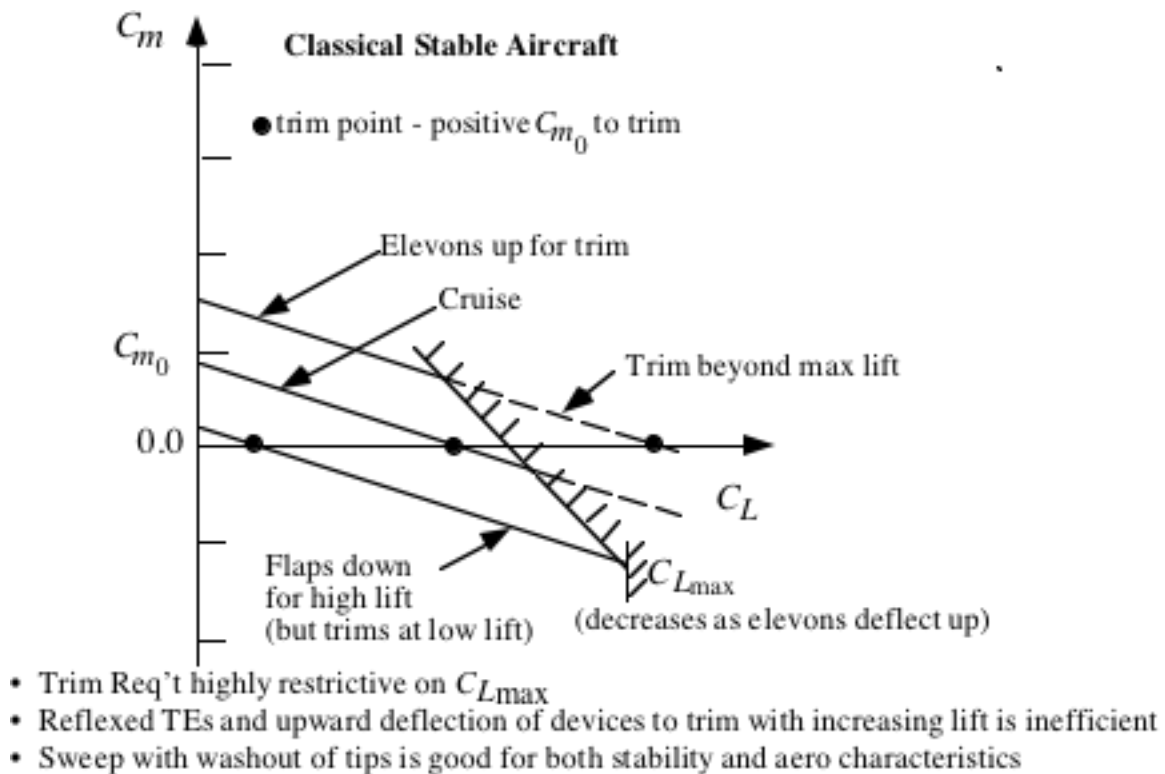


**Figure D-8  $L/D$  Variation with altitude**

7. Determine the neutral point of the B-2. Examine the available information, and estimate the static margin. Does your conclusion make sense?

Using the side-view in Fig. D-1, the  $cg$  location was estimated to be between 32.25 and 36 feet aft of the nose. This was done assuming a  $15^\circ$  angle between the landing gear and the  $cg$  location. With the neutral point determined from the vortex lattice method to be 32.7 feet aft of the nose, the low speed static margin ranges from 1.1% stable to 8.4% unstable. This is in the range that would be expected for a current advanced design.

Using these values, the  $C_m-C_L$  curves presented in Fig. D-9 were used to illustrate the setup and advantages of near neutral or negative static margins compared to classically stable designs. This figure is based on the paper by Sears.<sup>6</sup> The figure shows that the use of modern control system technology, allowing an unstable airplane, plays an important part in the reemergence of the flying wing concept.



a. stable flying wing relations

**Figure D-9. Pitching moment trim for a classical stable airplane.**

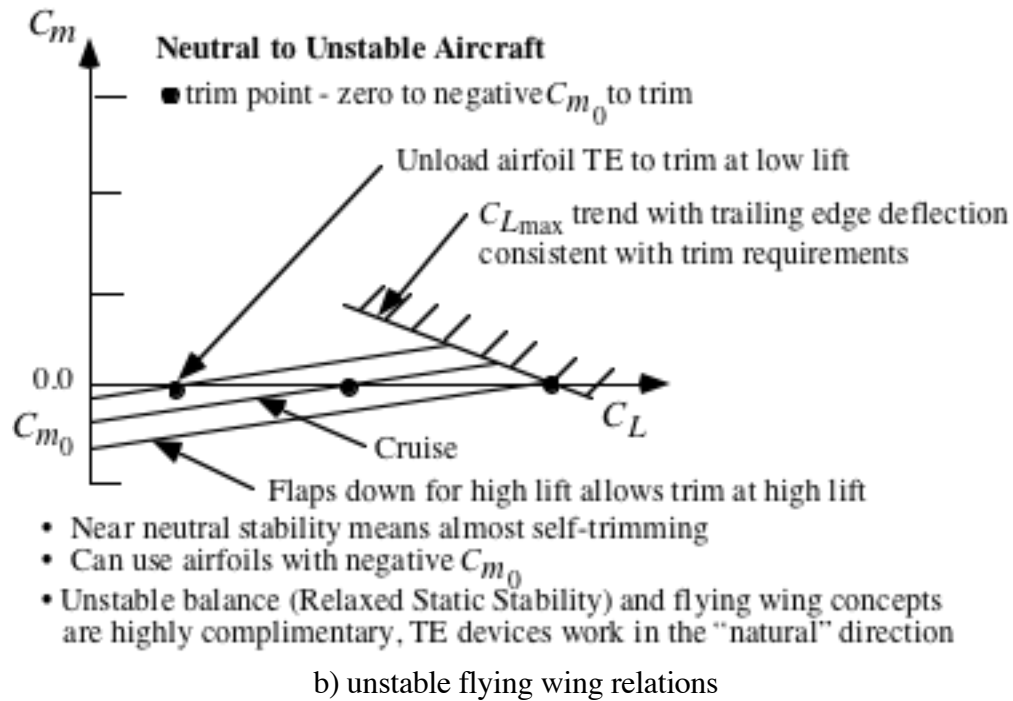


**Figure D-9. Comparison of stable and unstable aerodynamics of flying wing aircraft.**

The important outcome of studying Fig. D-9 is that a slightly unstable flying wing can trim at higher lift coefficients by deflecting the trailing edges down. This is in the right direction for achieving high lift for takeoff and landing. Thus relaxed static stability plays an important role in making the flying wing a practical concept.

The key lessons learned from this study:

- Aerodynamically, the B-2 spanload is surprisingly good considering the unusual planform.
- The students did not revisit the literature <sup>6, 7, 8, 9</sup> of the XB-35/YB-49 program, and thus missed an opportunity to fully appreciate the concept, and the role modern technology played in improving the feasibility of the concept

### D.3 Comparison of the Beech Starship and X-29

During the period from the late 1970s through the 1990s, canards concepts were popular. Burt Rutan was involved with Beech in developing the Starship. It had been recently certified when this project was carried out by the students. The objective was to try to understand the configuration concept, and canard concepts in general. The Grumman X-29 was a good example of a potential military canard configuration, and was used for comparison. The tools used for the B-2 study could be applied to these configuration. Table D-12 summarizes the work. Consider a number of sources of information available. Item 6 is a question your boss might ask, and expect an answer in “a day or so.”

**Table D-12. Starship and X-29 Study Questions**

1. Compare your estimate of the static margins for both the Beech Starship and the X-29.
2. Compare the load sharing between the canard and wing for the X-29 and the Starship. Consider a range of  $cg$ 's. What are the implications for selection of canard and wing airfoils?
3. Examine the control effectiveness of the canard. What is  $C_{m\delta c}$ ,  $C_{L\delta c}$ ? How do these numbers compare with a conventional layout competitor of the Starship?
4. With an untwisted wing, what is the span “ $e$ ” of the Starship? the X-29?
5. What is the twist distribution required to obtain a minimum drag spanload for the Starship? the X-29? Consider both the isolated wing case, and the wing in the presence of the canard.
6. Make your assessment. Is the Starship a better idea than other equivalent current aircraft (the Piaggio Avanti in particular)? How is the Starship concept different than the X-29. Why? Does that make the Starship a better or worse idea than the X-29? What do you advocate as the future trend for business aviation configurations from an aerodynamics standpoint?

The format is similar to the B-2 project, but now contains two lifting surfaces. In this case the key resource for geometry was Jane's<sup>10</sup>. The students were able to conduct their investigation without any additional information. The schematic of the planforms used in the project are shown in Figures D-10 and D-11. The estimates of center of gravity and neutral point are included. In the case of the Starship, the basic configuration was estimated to be about 10% stable. The X-29 was found here to be about 32% unstable. Thus the aerodynamic analysis results are consistent with the operation of each aircraft. The Starship does not use an advanced fly-by-wire flight control system, and is statically stable. In contrast, the X-29 exploits the advantages of an advanced flight control system to balance the aircraft at a significant level of static instability.

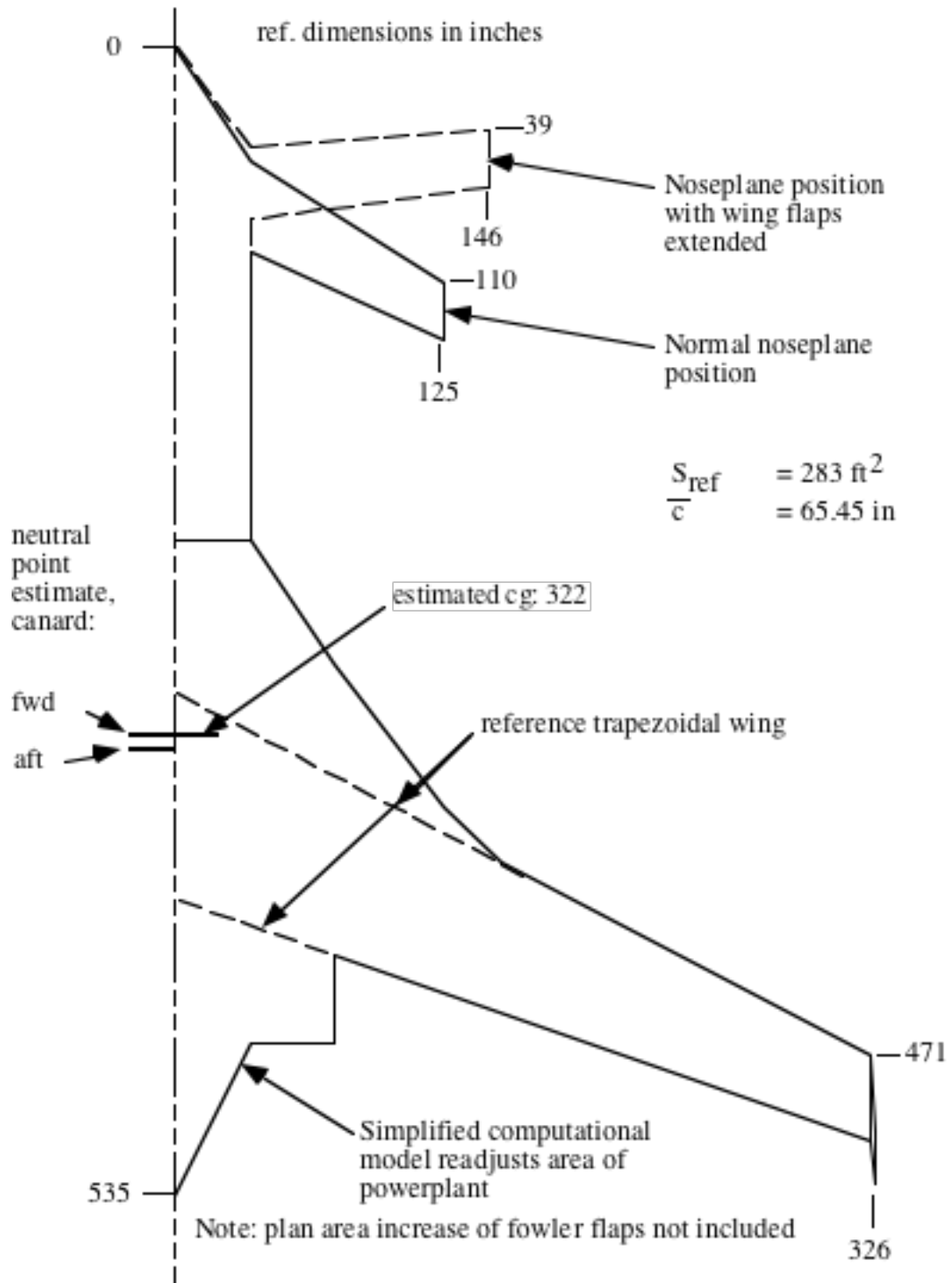


Figure D-10. Starship planform used for analysis.

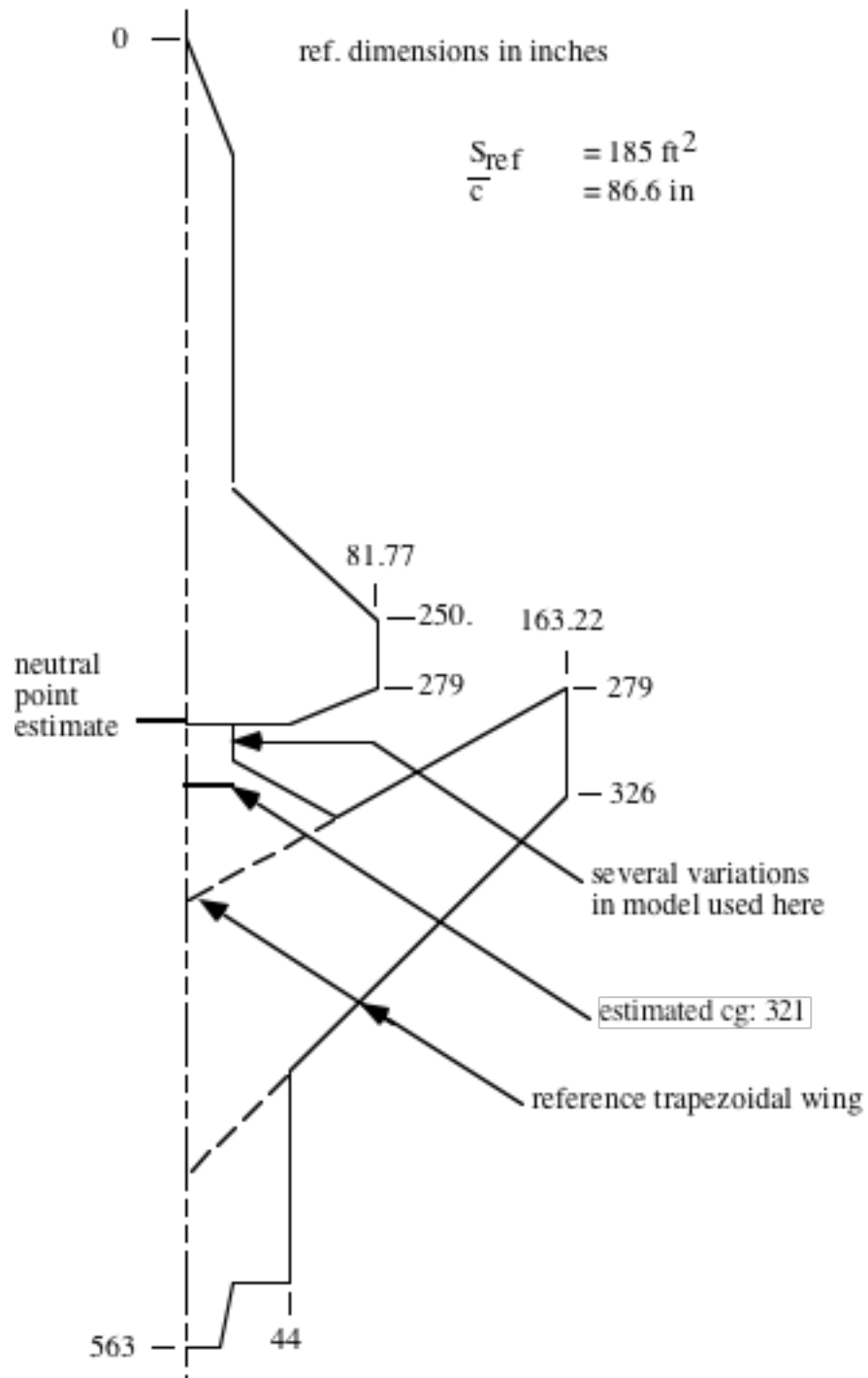


Figure D-11. Grumman X-29 configuration

Table D-13 contains the **VLMpc** data set developed using the information in Figure D-10. Table D-14 is the **VLMpc** data set for the X-29, created using Figure D-11.

**Table D-13 VLMpc model of the Starship**

Starship model			
2.	1.	1.0000	27193.
6.	0.	0.	0.00
0.0	0.0	0.0	1.
-54.	-35.		
-110.	-125.		
-137.	-125.		
-96.	-35.		
-230.	-35.		
-230.	0.0		
12.			
-230.	0.0		
-230.	-35.		
-288.	-74.		
-355.	-125.		
-381.	-152.		
-471.	-324.	85.	
-506.	-326.	0.	
-531.	-326.	85.	
-510.	-324.		
-424.	-74.		
-465.	-74.		
-465.	-35.		
-535.	0.0		
1.	9.	15.	.20
1.	0.	0.	0.
			0.
			0.

**Table D-14. VLMpc model of the X-29.**

X-29 vlm model			
2.	1.	1.0000	27193.
6.	0.	0.	0.00
0.0	0.0	0.0	1.
-50.	-20.		
-194.	-20.		
-250.	-81.771		
-279.	-81.771		
-295.	-44.0		
-295.	0.0		
10.			
-295.	0.0		
-295.	-20.		
-311.	-20.		
-335.	-64.		
-279.	-163.22		
-326.	-163.22		
-444.	-44.		
-535.	-44.		
-535.	-20.		
-563.	-14.		
-563.	0.0		
1.	9.	13.	.20
1.	0.	0.	0.
			0.
			0.

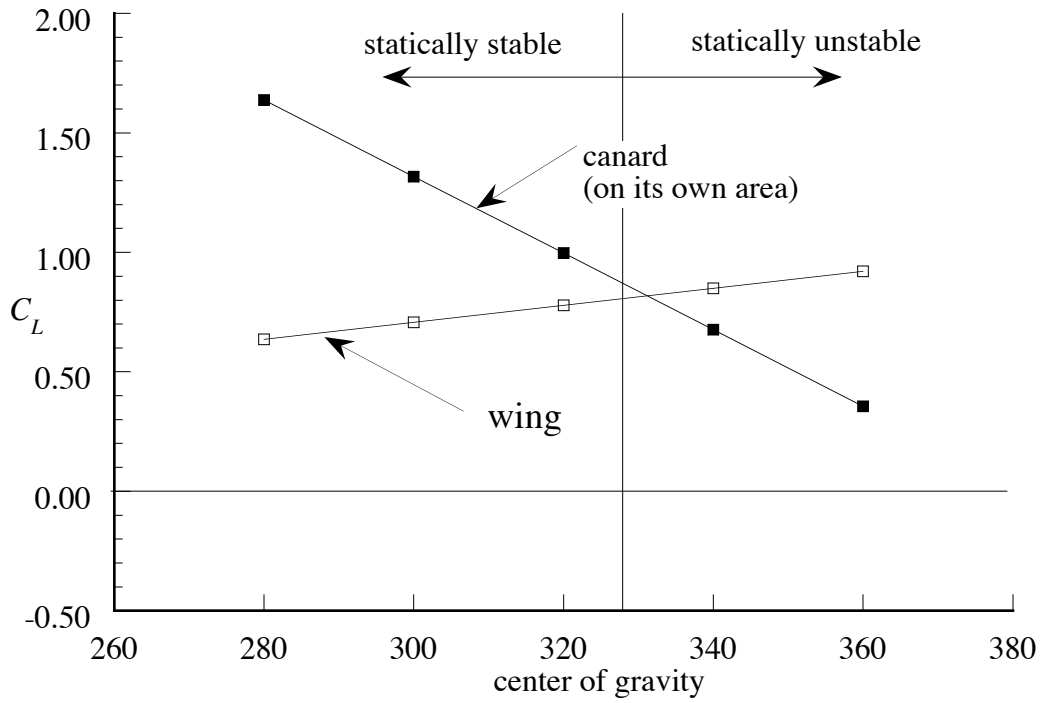
The forward position of the Starship canard, or foreplane, is connected to the extension of the fowler flaps. The additional area of the flaps was not estimated by students in this project, and the forward position leads to an approximately neutral static margin. According to Swanborough,<sup>11</sup> the area of the Fowler flap results in the stability level remaining the same as the canard moves forward. This feature illustrates the sophistication required to develop an aircraft concept. Figure D-12 shows a photo of the Starship taken at the Virginia Tech airport in the early 1990s.

Figure D-13 provides the load sharing requirements for trim between the canard and the wing for each aircraft. The results change with the center of gravity position. In the case of the Beech Starship, the requirement for a stable aircraft means the canard must always operate at a lift coefficient higher than the wing. When designed properly, this results in an airplane where the canard will always stall before the main wing. In the case of the X-29, the canard is at a significantly lower lift coefficient than the wing.

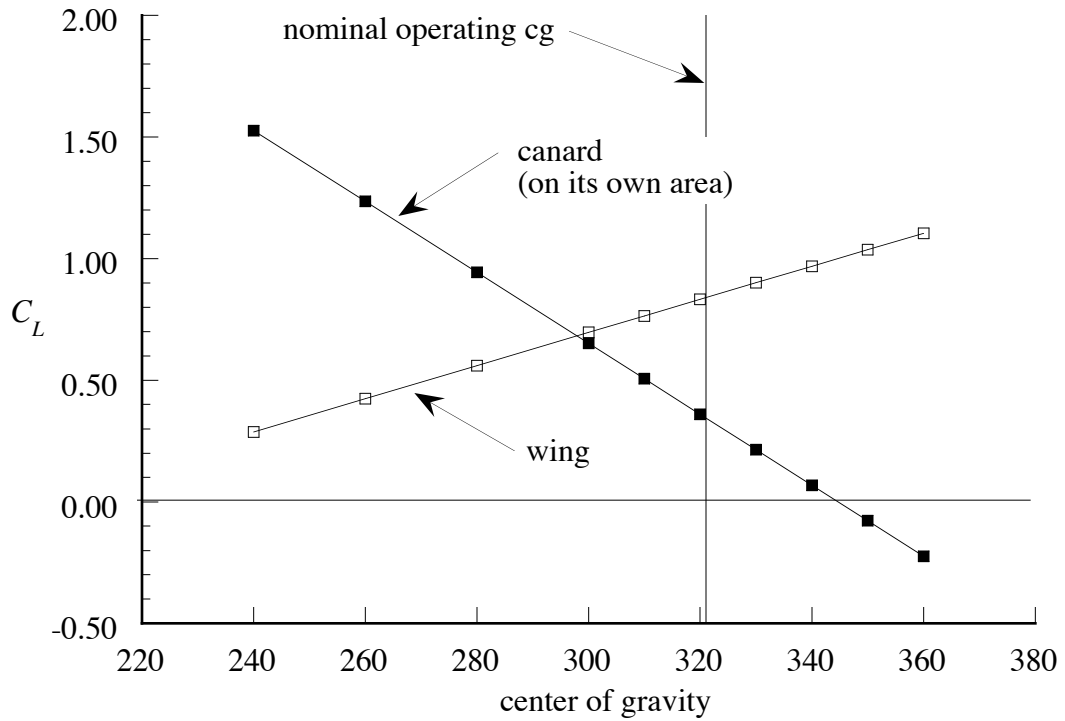


**Figure D-12. Beech Starship at the Virginia Tech Airport**

The choice of center of gravity location is important in obtaining the minimum trimmed induced drag. Figure D-14 shows the benefit of relaxed static stability technology. The center of gravity for minimum induced drag corresponds to a negative static margin. In Fig. D-14a the Starship is shown to be limited by stability requirements from reaching the highest cruise efficiency available for the configuration. In contrast, the X-29 is balanced at the edge of the minimum drag bucket. These approximate calculations were made using Lamar's design code LAMDES,<sup>12</sup> ignoring the limits to airfoil performance, which are also important.<sup>13</sup> This example requires that the induced drag be calculated considering the multiple-lifting surfaces and non-planar effects. **LAMDES** can be used as an extended version of **LIDRAG** to account for these effects.



a) Beech Starship



b) X-29

Fig. D-13. Load sharing requirements between the canard and wing.

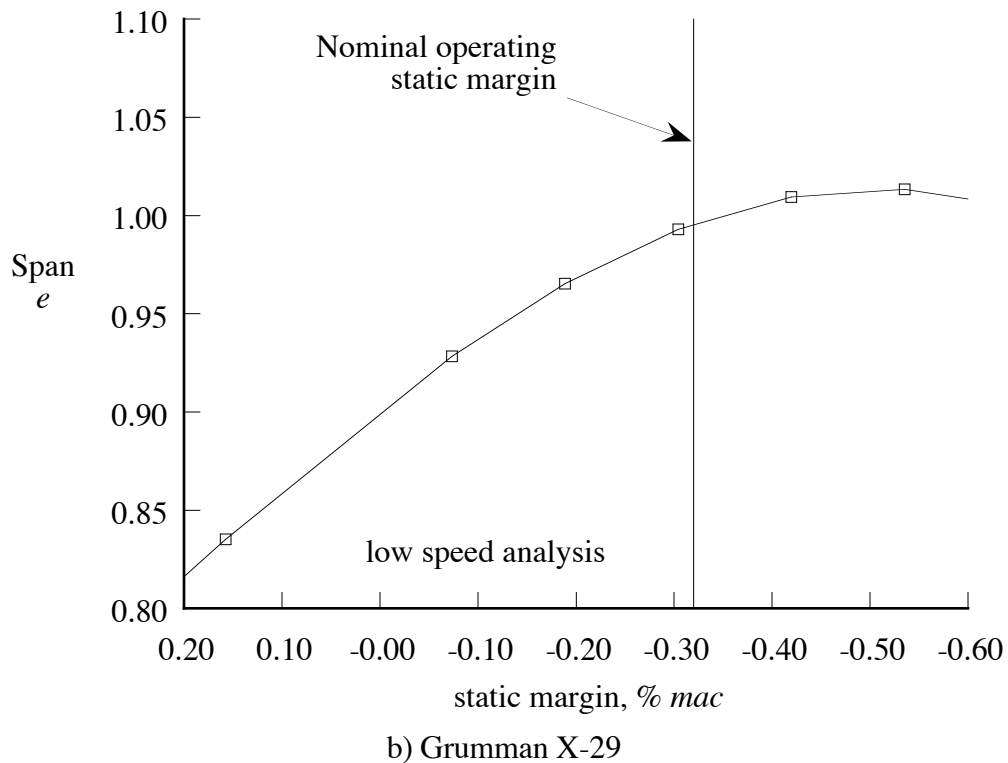
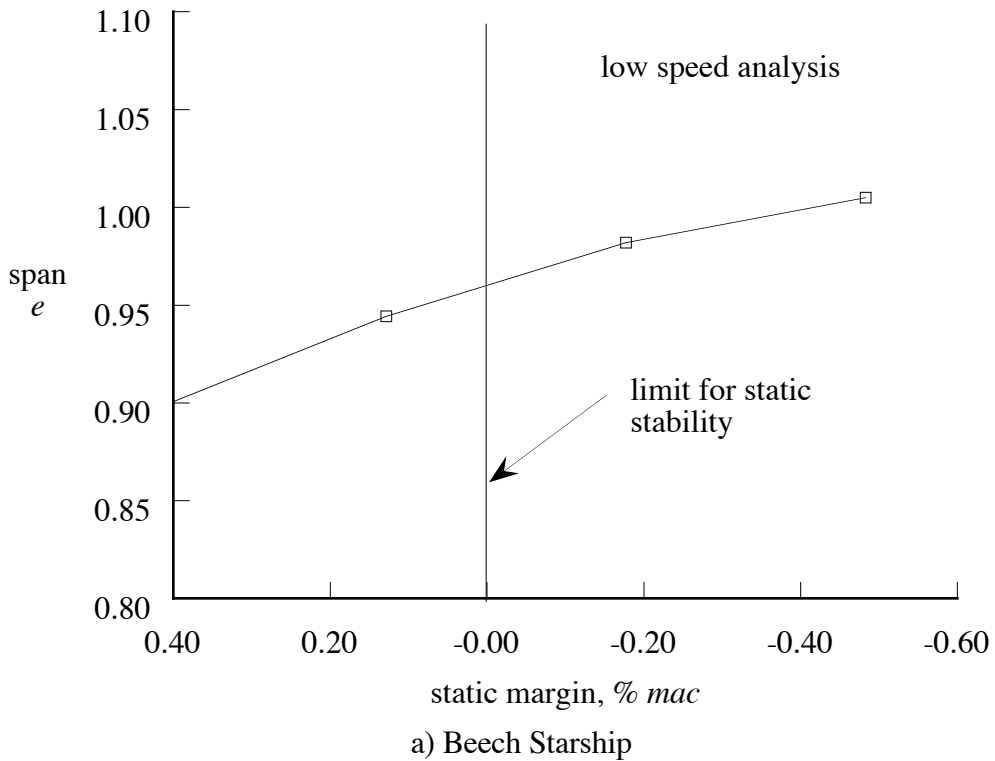


Figure D-14. Effect of trim requirement on lift induced drag using vortex lattice analysis.

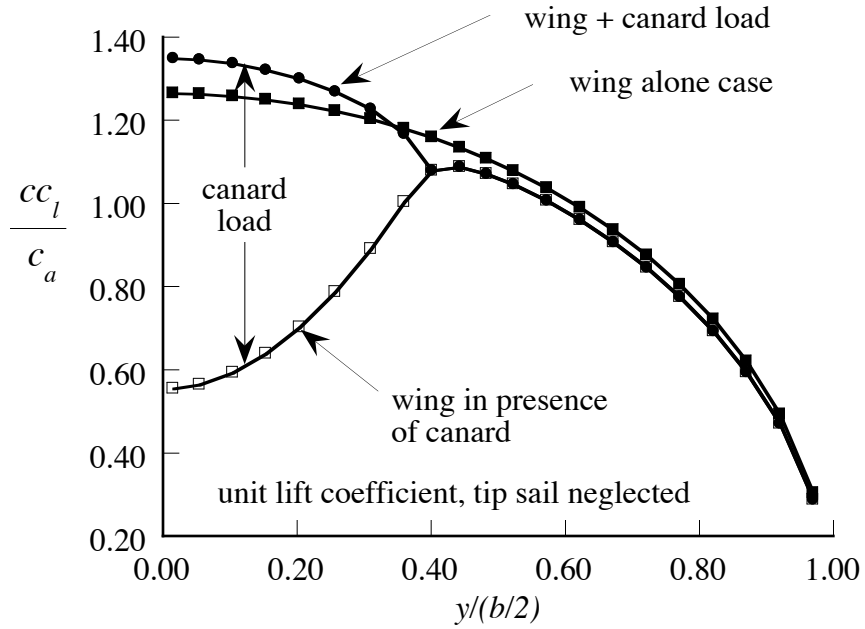
Canard effectiveness as a control is slightly unusual. The canard is an effective moment generator, but increasing the canard incidence does not produce an equivalent increase in configuration lift. In cases where linear theory aerodynamic theory is valid, the increased lift on the canard produces additional downwash on the wing. The result is a loss of lift on the wing roughly equal to the canard lift. In transonic and separated flow situations the linear aerodynamic flowfield model is not valid, and improved calculations or testing is required. Figure D-15 shows the X-29 on display at the U.S. Air Force Museum in Dayton, Ohio.

Figure D-16 shows the spanloads that correspond to the operation of the X-29 and Starship at their design points. Because the canard and wing are nearly coplanar, it is appropriate to combine them. Essentially, the vertical separation of the surfaces results in two distinct limits. In the first, the canard is coplanar with the wing, and the sum of the spanloads should be elliptic. As the vertical separation becomes large, individual spanloads should be elliptic. Most canard designs correspond to the first case, and this is evidenced in the results of an optimization, as shown in Fig D-16.

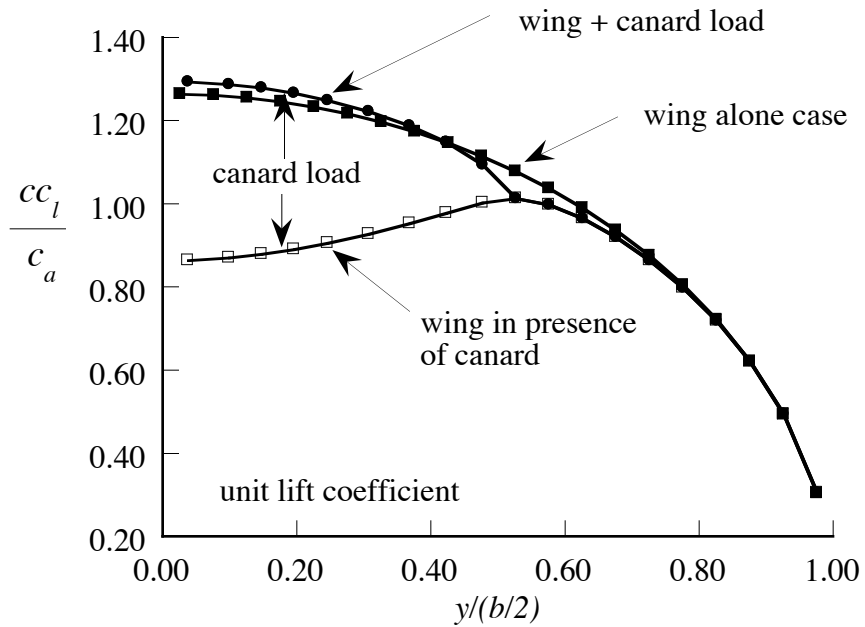
Figure D-17 gives the wing incidence distribution required to achieve the spanloads contained in Fig. D-16. This includes the basic angle of attack and additional twist. The design wing twist will change when the wing is in the wake of the canard. In this case, the canard wake is held flat and fixed, resulting in the most extreme condition. This shows how you need to compensate for flow nonuniformity in interacting flowfields. Note also that the trends in twist between aft and forward swept wings are exactly opposite. In particular, the presence of the canard reduces the twist variation required across the wing in the case of the X-29.



**Figure D-15 X-29 on display at the US Air Force Museum.**

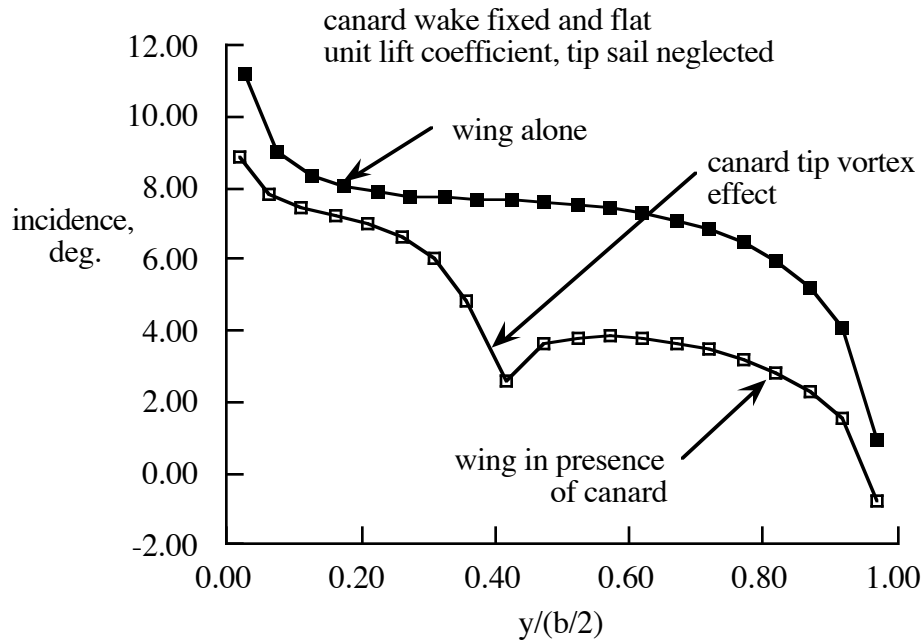


a) Beech Starship

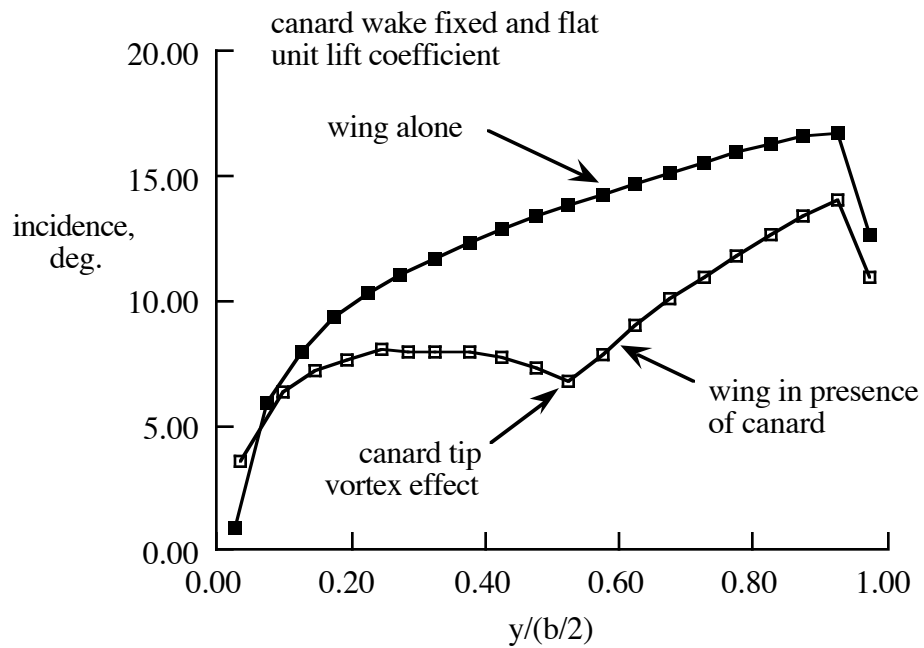


b) Grumman X-29

**Figure D-16. Minimum trimmed drag spanloads**



a) Beech Starship



b) Grumman X-29

**Fig. D-17. Incidence distribution required to achieve minimum drag spanloads presented in Fig. D-16.**

Additional information on the X-29 aerodynamic design is given in several papers.<sup>14, 15, 16, 17</sup> Many comparisons of forward/aft swept wings and canard/tail configurations have been published. Key reading should include McKinney and Dollyhigh,<sup>18</sup> Landfield and Rajkovic,<sup>19</sup> and McGeer and Kroo.<sup>20</sup>

The assessment also required consideration of a competitor aircraft, the Piaggio Avanti. In this case, the Aviation Week<sup>21</sup> article provided a useful analysis of the Starship and Avanti. Some confusion exists within the literature on the aerodynamics of three-surface configurations. The definitive analysis has been given in a NASA TP,<sup>22</sup> and the code is now available to students for future projects. The key benefit of a three surface configuration is the reduction in the trim drag variation with balance location.

The key lessons in this case study were that canard configurations go most naturally with unstable designs. If a canard aircraft is balanced to be stable, the canard airfoil design will likely be critical. Finally, trim is an important issue in the aerodynamic layout of aircraft.

### D.4 Term Project: Examine the YF-22 and YF-23

The US Air Force was in the process of selecting its new ATF - Advanced Tactical Fighter when this project was assigned. The selection was scheduled to be announced about the time the assignment was due. As luck would have it, the announcement was made on the exact day that the assignment was due. The objective was to make an assessment of the aerodynamic design of these two planes.

The assignment: Use all the tools we have from class, and explain how you used them. Reference other data sources used. Turn in an engineering report, including copies of input data sets as appendices. Use recent aviation magazines to establish a geometric model of each aircraft. Aviation Week during Fall 1990 is a good source.

1. Compare your estimate of the low speed static margins for both candidates. (review your notes from stability and control to recall definitions of SM and aircraft trim requirements)
2. Compare the load sharing between the tail and wing for the YF-22 and YF-23. Do this for both up and away flight and the approach condition. Consider a range of  $cg$ 's. What are the implications for selection of wing and tail airfoils?
3. Examine the control effectiveness of the tail. What is  $C_{m\delta t}$ ,  $C_{L\delta t}$ ?
4. What is the span " $e$ " for each plane with an untwisted wing?
5. What is the twist distribution required to obtain an elliptic spanload for each airplane? Consider both the isolated wing case, and the wing-tail case.
6. Using the analysis performed above, examine and discuss the trim drag issues. What if you used thrust vectoring to help trim?
7. Estimate the skin friction drag on each airplane.
8. Make your assessment. Would you pick the YF-22 or YF-23? Explain your choice, and comment on any refinements you would make.

This was a timely project. The students used the *Aviation Week*<sup>23</sup> and *Air International*<sup>24</sup> analysis and the book by Sweetman.<sup>25</sup> Again, the requirements were similar to the previous projects, with the addition of a requirement to consider the estimation of friction drag. This allowed the students to estimate the  $L/D$  of the airplanes. Although interesting, without explicit requests, this had not been done previously.

As luck would have it, the due date coincided with the Air Force announcement of the selection. As a result, the student interest was extreme. Interestingly enough, a number of their parents turned out to be employed by the DOD, and were able to supply an extraordinary amount of propaganda that was distributed by lobbyists.

The key lesson in this term project was that using the methods available in the course, both airplanes were nearly equal. Supersonic and low speed high angle of attack aerodynamic evaluations are required to make a selection. The student use of nonlinear analysis through airfoil design and analysis continued to be produce disappointing results.

### **D-5. Discussion**

The case studies presented in this Appendix show that a significant number of issues associated with configuration aerodynamics can be resolved without expensive CFD calculations. Students can get considerable insight, and make good sanity checks against much more sophisticated codes using a PC. However, other aspects of the problem require the use of sophisticated CFD methods. Still other aspects require wind tunnel or flight test at present. The role of each is identified with the use of these projects. These projects require an assessment intended to improve the student's ability for "critical thinking."

### **D-6. References**

---

<sup>1</sup> Mason, W.H., "Applied Computational Aerodynamics Case Studies," AIAA Paper 92-2661, June 1992.

<sup>2</sup> "USAF, Northrop Unveil B-2 Next-Generation Bomber," *Aviation Week & Space Technology*, Nov. 28, 1988, pp.20-27.

<sup>3</sup> *Air International*, Feb. 1989, pg. 104.

<sup>4</sup> Waaland, I.T., "Technology in the Lives of an Aircraft Designer," AIAA 1991 Wright Brothers Lecture, Sept 1991, Baltimore, MD.

<sup>5</sup> Miller, J., *Northrop B-2 Stealth Bomber*, Aerofax Extra 4, Specialty Press, Stillwater, 1991.

<sup>6</sup> Sears, W.R., "Flying-Wing Airplanes: The XB-35/YB-49 Program," AIAA Paper 80-3036, March 1980.

<sup>7</sup> Northrop, J.K., "The Development of the All-Wing Aircraft," 35th Wilbur Wright Memorial Lecture, *The Royal Aeronautical Society Journal*, Vol. 51, pp. 481-510, 1947.

<sup>8</sup> Woolridge, E.T., *Winged Wonders*, Smithsonian Institution Press, Washington, 1983.

<sup>9</sup> Coleman, T., *Jack Northrop and the Flying Wing*, Paragon House, New York, 1988.

- <sup>10</sup> Taylor, J.W.P., ed., *Jane's All the World's Aircraft 1988-89*, Jane's Group, Surrey, 1988.
- <sup>11</sup> Swanborough, G., "Starship ...bright newcomer in a conservative firmament," *Air International*, April 1991.
- <sup>12</sup> Lamar, J.E., "Application of Vortex Lattice Methodology for Predicting Mean Camber Shapes of Two-Trimmed-Noncoplanar-Complex Planforms with Minimum Induced Drag at Design Lift," NASA TN D-8090, June 1976.
- <sup>13</sup> Mason, W.H., "Wing-Canard Aerodynamics at Transonic Speeds - Fundamental Considerations on Minimum Drag Spanloads," AIAA Paper 82-0097, January 1982
- <sup>14</sup> Spacht, G., "The Forward Swept Wing: A Unique Design Challenge," AIAA Paper 80-1885, August 1980.
- <sup>15</sup> Moore, M., and Frei, D., "X-29 Forward Swept Wing Aerodynamic Overview," AIAA Paper 83-1834, July 1983.
- <sup>16</sup> Raha, J., "The Grumman X-29 Technology Demonstrator: Technology Interplay and Weight Evolution," SAWE Paper No. 1665, May 1985.
- <sup>17</sup> Frei, D., and Moore, M., "The X-29— A Unique and Innovative Aerodynamic Concept," SAE Paper 851771, October 1985.
- <sup>18</sup> McKinney, L.W., and Dollyhigh, S.M., "Some Trim Drag Considerations for Maneuvering Aircraft," *Journal of Aircraft*, Vol. 8, No. 8, Aug. 1971, pp.623-629.
- <sup>19</sup> Landfield, J.P., and Rajkovic, D., "Canard/Tail Comparison for an Advanced Variable-Sweep-Wing Fighter," *Journal of Aircraft*, Vol. 23, No. 6, June 1986, pp.449-454.
- <sup>20</sup> McGeer, T., and Kroo, I., "A Fundamental Comparison of Canard and Conventional Configurations," *Journal of Aircraft*, Vol. 20, No. 11, Nov. 1983. pp.983-992.
- <sup>21</sup> "...," Piaggio Avanti, Beech Starship Offer Differing Performance Characteristics," *Av. Wk. & Sp. Tech.*, Oct 2, 1989, pp75-78.
- <sup>22</sup> Goodrich, K.H., Sliwa, S.M., and Lallman, F.J., "A Closed-Form Trim Solution Yielding Minimum Trim Drag for Airplanes with Multiple Longitudinal Control Effectors," NASA TP 2907, May 1989.
- <sup>23</sup> Dornheim, M.A., "ATF Prototypes Outstrip F-15 in Size and Thrust," *Aviation Week and Space Technology*, Sept. 17, 1990, pp.44-50.
- <sup>24</sup> Braybrook, R., "ATF: The USAF's future fighter programme," *Air International*, Vol. 40, No. 2, Feb. 1991, pp.65-70.
- <sup>25</sup> Sweetman, B., *YF-22 and YF-23 Advanced Tactical Fighters*, Motorbooks, Osceola, 1991.